present by adding fluorescently labeled myosin, and looking for processive myosin runs that would indicate the presence of actin filaments, as described below (Fig. 5).

3.3 Myosin moves along actin filaments inside linear ZMWs

To observe myosin motility on polymerized actin filaments, we added fluorescently labeled myosin V and ATP to the ZMWs. We were able to see myosin V runs of >1 micron, as shown in the kymograph in Fig. 5, indicating that long actin filaments had been polymerized inside the linear ZMWs. Since myosin V steps are ~36 nm in length, this is long enough to allow at least 30 steps along actin inside the linear ZMWs.

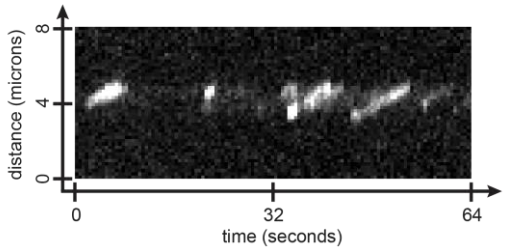

Fig. 5. Example kymograph of myosin V molecules walking along actin in a linear ZMW. Note that in some of the myosin runs shown in this kymograph, such as the one beginning around 5 seconds and the one beginning around 35 seconds, two myosin molecules are walking along the actin filament very close together.

3.4 Myosin walks in the flow-cell CLIC device under significant confinement

The CLIC imaging chamber confines molecules to a thin film to suppress background fluorescence. When the imposed confinement is on the same order as the molecular size, the confinement can alter molecular behavior. This was an important potential hurdle to overcome with CLIC, as it had not previously been demonstrated that the mechanical confinement introduced by the CLIC device was compatible with biological activity. In this work, we demonstrate the first biological application of CLIC by characterizing the processive movement of myosin along actin filaments at various degrees of confinement. This was an important step toward applying CLIC imaging to studying interactions of myosin with fluorescently labeled ATP at high concentrations. This characterization provides not only a technical measure of the potential improvement in imaging quality, but also insight into how confinement or crowding affects molecular interactions in this system and others.

The applied confinement, corresponding to the chamber height, is shown in Fig. 6(a). The contours of the least-squares fit to the interference pattern and dye fluorescence are superimposed on the data (see Methods Sect. 2.5).

The spatial distribution of actin filaments within the chamber was uniform, which was expected since the filaments were inserted before the chamber was compressed. The trajectories of individual myosin proteins at different locations in the chamber were imaged (e.g. Figure 6(b)). Figure 6(c) shows the area density at which we observed processive myosins as a function of the chamber height. Processive myosin movement was not observed in chambers with heights less than 58 nm (+ 6 nm/-12 nm; see Methods Sect. 2.7 for error analysis); instead, these motor proteins were either diffusing or immobile. Using the trajectories of motors that did undergo processive movement, the speed was calculated at different locations in the chamber. Little correlation was seen between velocity and chamber height, indicating that, if motile, the myosin movement is largely unperturbed by the confinement of the CLIC device (Fig. 6(d)). The chamber height measured by interferometry is the coverslip-coverslip separation, which exceeds the effective chamber height experienced by the proteins (e.g. due to surface-blocking agents, see Discussion).

#178943 - $15.00 USD Received 5 Nov 2012; revised 14 Dec 2012; accepted 15 Dec 2012; published 10 Jan 2013

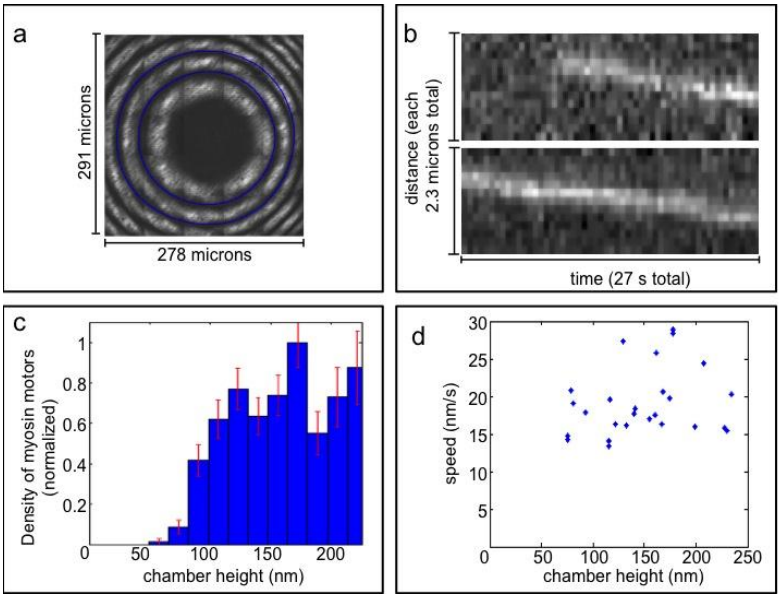

Fig. 6. Processive myosin movement is observed under confinement in the flow-cell CLIC device. (a) Interferometry of and least-squares fit to the CLIC imaging chamber height profile. The first two labeled interference minima (blue rings) correspond to heights of 184 nm and 368 nm respectively. (b) Two example kymographs of myosin proteins imaged in the chamber at heights of ~80 nm. (c) Distribution of the number of myosins exhibiting processive motion as a function of chamber height, normalized by area. Error bars represent the expected standard deviation assuming Poissonian counting statistics. (d) Scatter plot of processive motor speed vs. chamber height. The speed shows little correlation with chamber height, indicating that confinement does not significantly perturb the motor behavior at heights where motors continue to walk.

4. Discussion and conclusions

Both new technologies that we demonstrate, linear ZMWs and flow cell CLIC, show promise for single-molecule imaging of fluorescent molecules at higher concentrations than can be accessed via TIRF microscopy. This work represents and important advance, since, unlike other alternatives to TIRF, such as cylindrical ZMWs or nanoconfinement within vesicles or droplets, both of our techniques allow imaging of fluorescent molecules interacting with geometrically extended substrates. We have demonstrated here that processive molecular motors can be imaged with both novel technologies, under conditions that suppress background fluorescence in comparison to TIRF imaging and that do not alter the motor behavior. This is an important first step toward further biological applications.

Cylindrical ZMWs have already proven useful for observing single fluorophores at concentrations up to 10 μM [3], approximately 100-fold higher than TIRF, and the new geometry we present here will dramatically expand the types of experiments that can be used with this technology, allowing not only a fluorescence signal but also the location and movement of that fluorescent label (in one dimension) to be observed simultaneously. Though linear ZMWs may produce somewhat higher levels of background than have been demonstrated with circular ZMWs, due to their larger excitation volume in the linear dimension, they are still likely to allow single-molecule imaging with ~30-fold higher concentrations than TIRF.

Using flow cell CLIC imaging, we have demonstrated the first biological application of CLIC, showing that myosin motors can walk along actin filaments down to a chamber confinement as narrow as 60 nm. In the initial demonstration of CLIC imaging, at confinements narrower than about 300 nm, CLIC imaging was shown to improve the signal-

#178943 - $15.00 USD Received 5 Nov 2012; revised 14 Dec 2012; accepted 15 Dec 2012; published 10 Jan 2013

to-background in comparison to TIRF imaging [26]. Therefore, we expect that, at the confinements demonstrated in this study, implementing CLIC imaging will suppress the background from fluorophores in solution by at least five-fold, making single-molecule imaging possible at fluorophore concentrations at least five times higher than with TIRF. In fact, it may be that even further improvements are possible, since the BSA coating used to block both surfaces in this study may substantially increase the effective confinement experienced by molecules in the imaging chamber. While these concentration improvements are not as dramatic as those possible with ZMWs, they are significant, and CLIC has the advantage of the ease with which it may be implemented.

Thus, both technologies will have an important place, with ZMWs possibly more applicable to systems where large increases in concentration are needed, and CLIC useful when more modest concentration increases are sufficient but a simpler experimental setup is desirable. Though not employed in this study, the CLIC geometry has an additional imaging characteristic that is advantageous for some experiments: it extends typical diffusion-limited observation periods of small proteins from ~10 microseconds for ZMWs (or ~100 microseconds for TIRF) to ~seconds for CLIC imaging. These improvements to both suppressing background fluorescence and extending observation periods make a wide range of new biophysical measurements possible.

In conclusion, we have demonstrated two new microscopy technologies that will facilitate a wide range of new single-molecule studies of low affinity molecular interactions and dynamics, particularly with substrates where one dimension extends beyond 100 nm. We have already described one of the most obvious applications: looking at fluorescent nucleotide binding and releasing as processive motors move along filaments. There are many systems for which such an experiment will be informative, including the processive myosins, kinesins, and dynein. Another important application is in examining polymerization of biological filaments, such as actin. For instance, it has been suggested that actin may be able to undergo dynamic instability [32], analogous to that of microtubules. Although there is some evidence from experiments using TIRF that dynamics that are more transient and smaller in scale may occur in actin compared to those in microtubules [33,34], dynamic instability of actin has not been clearly observed experimentally. Imaging polymerization at higher concentrations of fluorescently labeled monomers will facilitate direct measurements of the polymerization and depolymerization kinetics of actin and of other biological filaments, such as microtubules or the many recently-discovered bacterial actin homologues [35].

Acknowledgments

MWE and JAS were supported by NIH Grant GM33289. MWE thanks the Gerald J. Lieberman Fellowship (Stanford University) for support. SRL thanks the Mary Feiser Fellowship (Harvard University) for support during early development of this work. SRL thanks NSERC EQPEQ 422513-12 and NSERC RGPIN 418915-12 for financial support of the presented CLIC microscopy (performed at McGill University). CM and JSL thank NSERC's Cellular Dynamics of Molecular Complexes CREATE Program for fellowship support. AEC was supported by NSF Grant CHE-0910824 and by the Harvard Materials Research Science and Engineering Center (MRSEC) under grant DMR-0820484. The authors thank Daniel Berard for assistance with flow cell preparation and for preparing the device schematic in Fig. 3 and Blair Jia for experimental assistance with flow cell preparation in the Leslie laboratory.

Statement of competing financial interests

JK is a full-time employee at Pacific Biosciences, a company commercializing single-molecule, real-time nucleic acid sequencing technologies.

#178943 - $15.00 USD Received 5 Nov 2012; revised 14 Dec 2012; accepted 15 Dec 2012; published 10 Jan 2013